

## 치아교정용 NiTi 아치 와이어의 부식특성에 미치는 폴리머 코팅의 영향

조주형<sup>1</sup>, 고영무<sup>1</sup>, 최한철<sup>1\*</sup> and William A. Brantley<sup>2</sup>

<sup>1</sup>조선대학교 치과대학 치과재료학교실, <sup>2</sup>오하이오 주립대 치과대학

### Effect of Polymer Coating on the Corrosion Characteristics of Nickel-Titanium Orthodontic Archwire

Joo-Young Cho<sup>1</sup>, Yeong-Mu Ko<sup>1</sup>, Han-Cheol Choe<sup>1\*</sup> and William A. Brantley<sup>2\*</sup>

<sup>1</sup>Department of Dental Materials, Research Center of Nano-Interface Activation for Biomaterials & Research Center for Oral Disease Regulation of the Aged, Chosun University, Gwangju, Korea, <sup>2</sup>Division of Restorative, Prosthetic and Primary Care Dentistry, College of Dentistry, Ohio State University

(Received: Jun 19, 2013; Revised: Jun 25, 2013; Accepted: Jun 25, 2013)

#### ABSTRACT

본 연구는 NiTi 교정용 와이어의 부식특성에 미치는 폴리머코팅의 영향에 관하여 연구한 논문으로 교정용 와이어에 페릴린을 코팅하여 표면분석장비와 전기화학적인 부식시험을 통하여 다음과 같은 결과를 얻었다. 코팅된 표면은 작은 코팅 입자가 뭉쳐있는 모양을 보였으며 그 두께는 약 20  $\mu\text{m}$ 를 보였다. 표면 거칠기는 코팅되지 않은 경우는 0.381  $\mu\text{m}$ 를 코팅한 경우는 4.70  $\mu\text{m}$ 를 나타내었다. 공식전위는 코팅하지 않은 경우가 1240 mV를, 코팅한 경우는 공식전위가 나타나지 않았다. 300 mV에서 전류밀도는 코팅하지 않은 경우가  $2.99 \times 10^{-6}$  A/cm<sup>2</sup>를, 코팅한 경우가  $2.13 \times 10^{-7}$  A/cm<sup>2</sup>를 각각 나타내었다. 정전위나 정전류 실험으로부터 내식성은 코팅한 경우가 증가하는 경향으로 나타났다.

**KEY WORDS** : Esthetic orthodontic wire, Surface morphology, Plasma polymer coating, Pitting potential, Corrosion resistance

## INTRODUCTION

Esthetic orthodontic treatment is available using ceramic or polymeric brackets and coated metallic wires so that these orthodontic appliances have appearances that match the shades of teeth. Gold alloy wires were originally used for orthodontics, but these have been replaced by base metal wires for many decades. The first base metal orthodontic wires were stainless steel and cobalt-chromium-nickel (Elgiloy), but subsequently introduced nickel-titanium wires (termed NiTi wires, because of their near-equiatomic NiTi composition) and beta-titanium wires have become clinically popular since their lower values of elastic modulus provide the desired lighter forces for tooth movement [1]. Orthodontic wires and brackets should exercise appropriate biomechanical force on teeth to enable rapid and

accurate tooth movement without damage to surrounding tissues during orthodontic treatment. However, loss of orthodontic force occurs from friction between the archwires and brackets during tooth movement. The numerous factors that affect these frictional losses are the bracket material and its surface condition [2]; the wire alloy and cross-section dimensions [3]; the types of ligating agent and ligation method; the bracket slot size and width [4]; the direction of orthodontic force application; and environmental elements such as saliva, dental plaque and corrosion [5].

However, metal archwires lack the esthetic tooth-color appearance desired by patients, and the orthodontic force from a coated metal archwire can be substantially decreased by the coating thickness. Moreover, many NiTi wire products being used widely are very sensitive to the manufacturing process or clinical user environment,

and their orthodontic force depends on temperature and stress, which can cause phase transformation from martensite to austenite [1,6]. To improve the esthetics of metal wires, some manufacturers have developed polymer-coated wires and metal-coated wires which are commercially available. However, when performing wire drawing and subsequent esthetic polymer coating on a NiTi product that is sensitive to temperature and stress, many manufacturing processes are involved that can affect the phase transformation behavior: (1) permanent deformation and heat treatment steps during the wire drawing, and (2) subsequent heat treatment during the coating procedure. For example, in esthetic polymer-coated superelastic [1] NiTi wire used for orthodontic treatment, there should be minimal change in the superelastic force delivery and archwire-bracket friction from the presence of the coating layer. There are a few reports on corrosion of coated archwire with manufacturing process. Therefore, in this study, new information is reported about the surface morphology, microstructural phases, and corrosion characteristics of an orthodontic NiTi wire that has an esthetically pleasing polymer coating.

## MATERIALS AND METHODS

The commercial rectangular 0.016 × 0.022 inch NiTi wire (Ni-Ti<sup>®</sup>) selected for the present study is manufactured by Ormco (Glendora, CA, USA) and is shown in Fig. 1(a). Prior to the coating process, the as-received wire surface was first treated by chemical etching, and then heat treatment was performed at 120°C for 4 h in 10 mTorr vacuum to minimize the occurrence of hydrogen embrittlement. To increase the adhesive property for the polymer coating, silver plating of about 3 μm thickness was deposited onto the surface, and heat treatment was performed again at 120°C for 4 h in 10 mTorr vacuum. The tooth-colored polymer (parylene) was applied by plasma deposition (Dany Harvest, Co) at room temperature for 4 h in 15 mTorr vacuum to yield a coating thickness of about 20 μm. To minimize physical property changes and increase the adhesion of the polymer, a final heat treatment of the coated wire was performed

at 130°C for 2 h in 10 mTorr vacuum.

The surfaces of the NiTi wire in the as-received condition and after polymer coating were observed with a metallographic microscope and a field-emission scanning electron microscope (FE-SEM), as well as analyzed by X-ray diffraction (XRD), to investigate the surface morphology and the phases present before and after the polymer coating, respectively. Elemental compositions of the wire and coating were obtained using energy dispersive X-ray spectroscopy (EDS). Using laser 3D-surface microscopy (Veeco NT800), the arithmetic average ( $R_a$ ) and maximum ( $R_{max}$ ) values of surface roughness were measured, along with the quadratic mean roughness ( $R_q$ ).

Electrochemical corrosion testing by cyclic potentiodynamic polarization was performed with a potentiostat (PARSTAT 2273; EG&G, USA). The electrolyte was de-aerated 0.9% NaCl at 36.5°C ± 1°C; a saturated calomel electrode (SCE) was the reference electrode, and the prepared specimen was the working electrode. The distance between the specimen and reference electrode was adjusted to about 1 mm, and a high-density graphite electrode served as the counter electrode. To obtain the corrosion curve, potentiodynamic polarization was first conducted over the potential range from -1500 mV to +2000 mV for the forward scan and subsequently from +2000 mV to -1000mV for the reverse scan. A scan rate of 100 mV/min was used, and tests were performed at 36.5°C ± 1°C. To evaluate pitting behavior and stability of the polymer-coated wire surface, galvanostatic and potentiostatic tests were performed at 300 mV potential and 0.0001 mA/cm<sup>2</sup> current density, respectively, in the same electrolyte after de-aeration with pure argon. Morphologies of the non-coated and coated specimens after corrosion testing were observed using FE-SEM.

## RESULTS AND DISCUSSION

Figure 1 shows the (a) as-received and (b) polymer-coated NiTi wire surfaces, respectively. The polymer-coated surface had a tooth color appearance. Surfaces of the rectangular wire had uniform coating on the curvature area, and scratches from the manufacturing

process were covered by the coating, providing good esthetics for the wire [2,7].

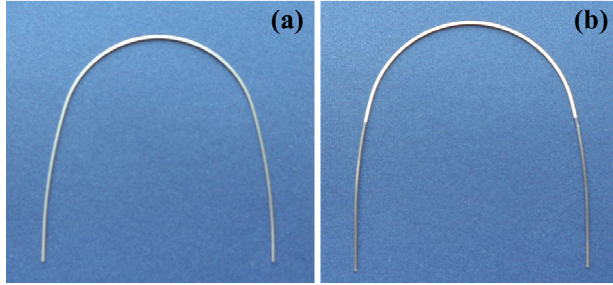


Figure 1. The samples used in this study. (a) non-coated wire; (b) polymer-coated wire.

Figure 2 shows details of the non-coated and polymer-coated surfaces observed with the FE-SEM. Processing defects in non-coated rectangular wires, Fig. 2 (a) and (b), were absent when the polymer-coated wires were examined at high magnification, Fig. 2 (c) and (d). These defects affect the wire surface roughness during orthodontic treatment of the teeth, causing some loss of orthodontic force due to increased friction with brackets, and these defects may decrease the biocompatibility of the wire in the oral environment. It is evident that most of the surface defects from manufacturer processing have disappeared for the coated wires, with the appearance now controlled by the coating material [8].

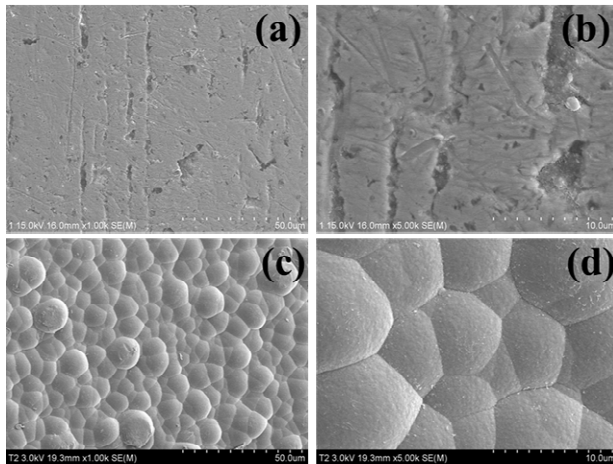


Figure 2. FE-SEM images showing non-coated and coated NiTi wires. (a) and (b), non-coated surface; (c) and (d), coated surface.

Figure 3 shows the XRD peaks from the non-coated

and polymer-coated surfaces. For the non-coated NiTi wire surface, weak peaks for martensite [1] or R-phase [9] and strong peaks for austenite [1] were observed, whereas for the polymer-coated surface, the peaks of austenite and silver were observed but martensite or R-phase peaks were not detected [10]. The commercial Ni-Ti<sup>®</sup> product is a superelastic wire with an austenite-finish temperature above mouth temperature, and is expected to consist of mainly austenite with some R-phase or martensite at room temperature [11]. Thus, the temperature-time regimen for the polymer-coating process may result in disappearance of the martensitic NiTi phase, at least from the near-surface region that is analyzed by x-ray diffraction [1], although a conclusive statement is not possible because of the weak martensite or R-phase peaks in the as-received (non-coated) wire.

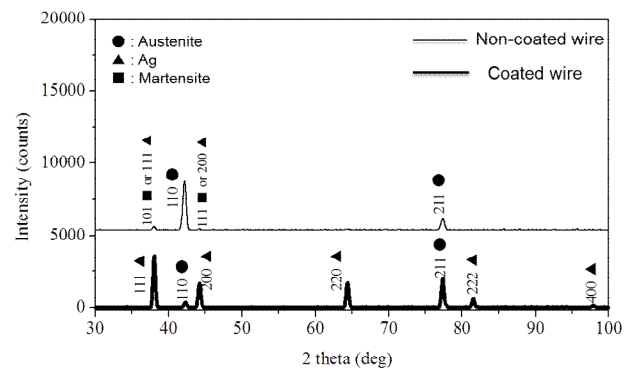


Figure 3. XRD peaks from non-coated and coated NiTi wire.

Figure 4 (a) shows a cross-sectional image of the coating layer on the orthodontic wire, and Fig. 4(b) presents the results of an EDS analysis for the coating surface. The surface of the polymer coating has the appearance of coalesced particles, and the coating thickness is about 20 $\mu$ m. The coating covers the surface scratches and other surface defects created during the original wire manufacturing process, and this should increase the biocompatibility and surface stability of the NiTi wire. The detection of Ag on the surface by EDS is a consequence of the silver coating process employed to increase the adhesiveness between the NiTi alloy surface and polymer coating. (Because of their low atomic weights, the principal elements

carbon and hydrogen in the polymer are not detected.) EDS analysis of the coating cross-section revealed the presence of S, which was attributed to the coating process, along with Ag [10].

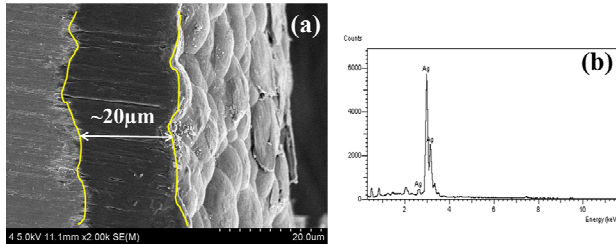


Figure 4. FE-SEM results showing (a) image of coated layer and (b) EDS peaks from coating on NiTi wire.

Figure 5 compares the three-dimension roughness of the non-coated and polymer-coated surfaces obtained by laser microscopy. When the coating procedure is completed, most of original manufacturer processing defects have been covered and the surface roughness depends on the coating material, as shown Fig. 2 (c) and (d). The roughness of the finished coating may have significant effects on the intensity of reflected light or surface abrasivity, even when the metal and polymer have the same value of roughness. The mean surface roughness ( $R_a$ ) was  $0.381 \mu\text{m}$  for the non-coated wire and  $4.70 \mu\text{m}$  for the coated wire, so the roughness of the coated wire is approximately 12 times lower than for the non-coated wire, a considerable improvement in surface roughness which should have clinical importance [2].

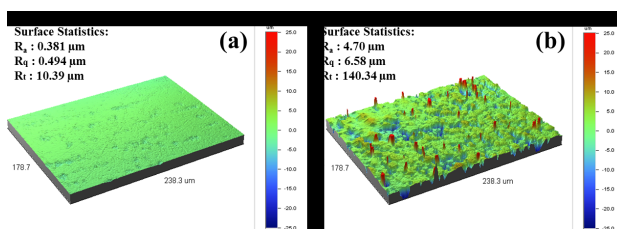


Figure 5. 3D laser morphologies showing the (a) non-coated and (b) coated surfaces of NiTi wire.

Figure 6 presents the cyclic potentiodynamic polarization (CPP) curves for non-coated and coated wires. While the general appearances of the CPP curves for non-coated and coated wires are similar, there are

important quantitative differences. For the uncoated wire, severe corrosion and pitting occurs at 1240 mV potential in the CPP curve. This behavior is thought to be greatly influenced by the presence of defects caused by severe localized damage at the affected areas during the wire processing. The dissolution on the metal surface is usually accelerated in the areas where surface defects, such as scratches, pores, precipitates, grain boundaries and impurities, are present [12]. Therefore, the corrosion resistance of the coated wire was increased because the scratches were covered by the coating. In contrast, a sudden pitting potential ( $E_{pit}$ ), corresponding to a well-defined localized breakdown and rapid increase in corrosion current over several decades, was not observed in the coated wire. In the mouth, the pitting potential for an orthodontic wire must be high compared to 300 mV which is considered to be the potential of concern [13]. According to the ISO standard [14], generally the corrosion test for a clinically acceptable metallic material should indicate the presence of a stable passive film at 300 mV. The corrosion resistance at the coating thus increased substantially, demonstrating that its corrosion performance is not adversely affected by the oral environment.

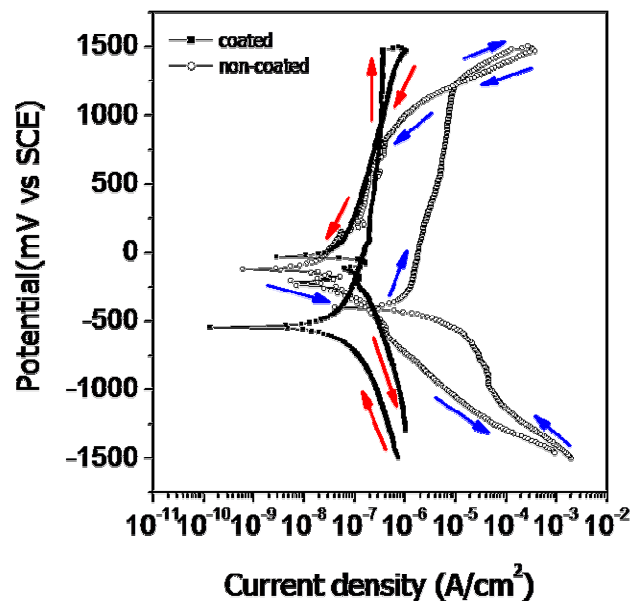


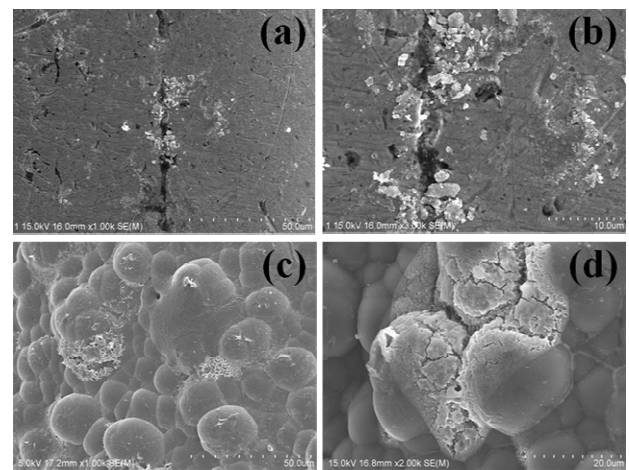
Figure 6. Cyclic potentiodynamic polarization curves of non-coated and coated Ni-Ti wire for testing in 0.9% NaCl solution at  $36.5^\circ \pm 1^\circ \text{C}$ .

**Table 1.** Electrochemical parameters of NiTi wires from cyclic potentiodynamic polarization curves for as-received (non-coated) surface and polymer-coated surface.

Wire Surface	Forward scan				Reverse scan		
	$E_{\text{corr}}$ (mV)	$I_{\text{corr}}$ (A/cm <sup>2</sup> )	$E_{\text{pit}}$ (mV)	$I_{300\text{mV}}$ (A/cm <sup>2</sup> )	$E_{\text{corr}}$ (mV)	$I_{\text{corr}}$ (A/cm <sup>2</sup> )	$I_{300\text{mV}}$ (A/cm <sup>2</sup> )
Non-coated	-400	$4.2 \times 10^{-8}$	1240	$2.99 \times 10^{-6}$	-120	$6.00 \times 10^{-10}$	$1.42 \times 10^{-7}$
Coated	-540	$1.4 \times 10^{-10}$	-	$2.13 \times 10^{-7}$	-30	$2.86 \times 10^{-9}$	$1.11 \times 10^{-7}$

From Table 1, for the intraoral potential at 300 mV, the current density for the forward scan decreased substantially from  $2.99 \times 10^{-6}$  A/cm<sup>2</sup> for the uncoated wire to  $2.13 \times 10^{-7}$  A/cm<sup>2</sup> for the coated wire, showing the large effect of the polymer coating on corrosion behavior. For the coated wire, the CPP curve was shifted beneficially to the left and down, compared to the CPP curve for the non-coated wire (Fig. 6). Comparing the pitting resistance quantitatively from the forward scan results, for the non-coated wire the corrosion potential ( $E_{\text{corr}}$ ) is -400 mV and the pitting potential is 1240 mV, and thus the pitting resistance  $|E_{\text{pit}} - E_{\text{corr}}|$  is 1640 mV (Table 1). For the coated wire, the corrosion potential is -540 mV and a pitting potential was not observed on the CPP curve, so that a pitting resistance  $|E_{\text{pit}} - E_{\text{corr}}|$  could not be defined; the pitting resistance is much greater than that for the non-coated wire. As mentioned earlier, this difference in pitting resistance is attributed to the presence of manufacturer processing defects on the surface that are not covered by the polymer coating.

Figure 7 shows the corrosion morphology of the non-coated (a, b) and coated surfaces (c, d). Severe pitting corrosion was observed around scratches in the non-coated wire. For the coated wire, pitting was also observed on the surface, indicating that the coating layer was degraded by presumably the penetration of  $\text{Cl}^-$  ions from the electrolyte. It is evident from Fig. 2 (c) and (d) that corrosion is accelerated at the boundary of the coating and wire, and at crevices in the coating [12]. The morphology at these corroded regions agrees well with the characteristics of the CPP curves.

**Figure 7.** FE-SEM images showing corrosion morphology of non-coated (a, b) and coated surfaces (c, d) of NiTi wire after potentiodynamic polarization test in 0.9% NaCl solution at  $36.5 \pm 1^\circ \text{C}$ .

Figures 8 and 9, respectively, compare the current density-time curves at 300 mV potential and the potential-time curves at 0.0001 mA/cm<sup>2</sup> current density for the non-coated and coated wires. The current density decreased as time increased due to formation of a passive oxide film on the surface, as shown in Fig. 8. It can be seen that at longer times the current density for the non-coated wire was higher than that for the coated wire. From the potential-time curves in Fig. 9, the potential increased as time increased, and the potential of the coated wire was higher than that of non-coated wire (except at very short times). These results confirm our previous report that coated wire has superior pitting corrosion resistance compared to the non-coated wire [10].

The foregoing results establish that suitable esthetics was obtained by the polymer coating on the surface of the NiTi wire and that the corrosion resistance of

the coated wire was substantially increased. For the non-coated wire, severe metal dissolution occurred at surface defects caused by manufacturer processing. In order to perform optimum coating on NiTi wires, the surface quality of the starting non-coated wire from the manufacturer needs to be improved.

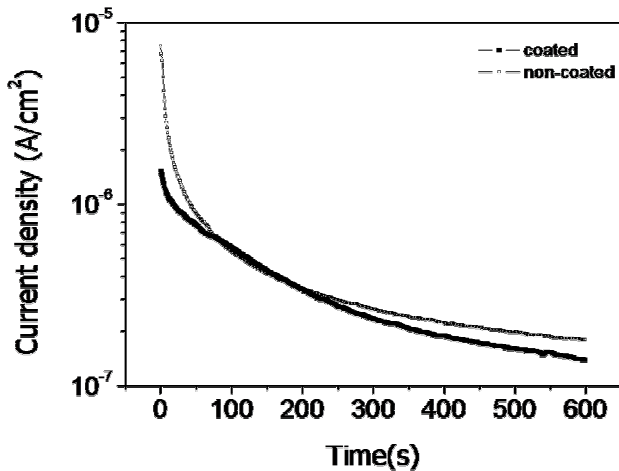


Figure 8. Current density-time curves of non-coated and coated NiTi wire after potentiostatic testing at constant 300 mV potential in 0.9% NaCl solution at  $36.5 \pm 1^\circ C$ .

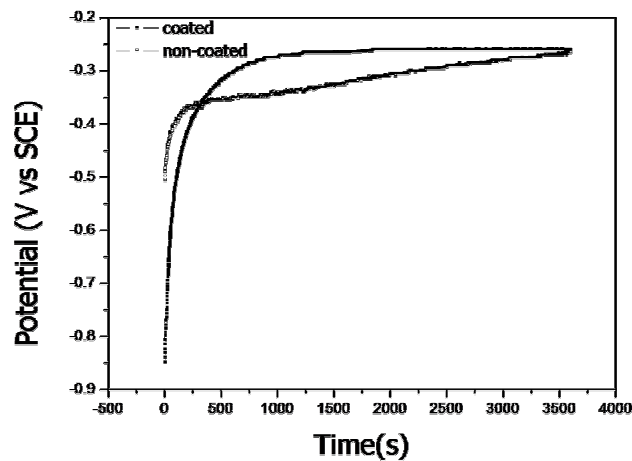


Figure 9. Potential-time curves of non-coated and coated NiTi wire after galvanostatic testing at constant  $0.0001 \text{ mA/cm}^2$  current density in 0.9% NaCl solution at  $36.5 \pm 1^\circ C$ .

## CONCLUSIONS

For non-coated NiTi wire, many processing defects from the manufacturing were observed on the surface, and when the polymer coating was performed, the processing defects were covered. For the non-coated

superelastic wire surface, X-ray diffraction peaks from martensite/R-phase and austenite were detected, whereas for the polymer-coated surface, peaks from austenite and silver (used to improve coating adhesion) were detected but not peaks from martensite/R-phase. The coated surface has the appearance of small coalesced particles, and the coating thickness was about  $20 \mu\text{m}$ . The surface roughness ( $R_a$ ) was  $0.381 \mu\text{m}$  for the non-coated wire and  $4.70 \mu\text{m}$  for the coated wire. The pitting potentials of the non-coated and coated wires were 1240 mV and non-defined, respectively. The current density at 300 mV potential was decreased considerably from  $2.99 \times 10^{-6} \text{ A/cm}^2$  for non-coated wire to  $2.13 \times 10^{-7} \text{ A/cm}^2$  for coated wire. The corrosion potential ( $E_{\text{corr}}$ ) was  $-400 \text{ mV}$  for non-coated wire and  $-540 \text{ mV}$  for coated wire. In case of non-coated wire, the current density-time curve was higher than that of coated wire, whereas the potential-time curve of coated wire was higher than that of non-coated wire.

## REFERENCES

Brantley WA (2001). Orthodontic Materials: Scientific and Clinical Aspects, Eliades T. (ed), Thieme, pp. 52-84.

Iijima M, Muguruma T, Brantley WA, Choe HC, Nakagaki S, Alapati SB, Mizoguchi I (2012). Effect of coating on properties of esthetic orthodontic nickel-titanium wires. Angle Orthod 82:319-325.

Kapila A, Angolkar PV, Duncanson MG, Nanda RS (1990). Evaluation of friction between edgewise stainless steel brackets and orthodontic wires of four alloys. Am. J. Orthod 98:117-126.

Frank CA, Nikolai RJ (1980). A comparative study of frictional resistances between orthodontic bracket and arch wire. Am. J. Orthod 78:593-609.

Stannard JG, Gau JM, Hanna MA (1986). Comparative friction of orthodontic wires under dry and wet conditions. Am. J. Orthod 89:485-491.

Andreasen G, Heilman H, Krell D (1985). Stiffness changes in thermodynamic Nitinol with increasing temperature. Angle Orthod 55:120-126.

Cho JY, Kim WG, Choi HS, Lee HJ, Choe HC (2010).

- Surface Characteristics of Polymer Coated NiTi Alloy Wire for Orthodontics. *J. Kor. Inst. Surf. Eng* 43: 132-141.
- Kim WG, Cho JY, Choe HC, Lee HJ (2010). Electrochemical Characteristics of Tooth Colored NiTi Wire. *Corros. Sci. Technol* 9:223-232.
- Riva G, Vanelli M (1995). A new calibration method for the X-ray powder diffraction study of shape memory alloys. *T. Airoldi, Phys. Stat. Sol A*148: 363-372.
- Brantley WA, Iijima M, Muguruma T, Choe HC, Nakagaki S, Alapati SB, Mizoguchi I, Kim I, Kim TS, Cheong HK, *J. Dent Res.* 90 Spec. Iss. A (2011) Abstract no. 45. (Available at [www.iadr.com](http://www.iadr.com)).
- Bradley TG, Brantley WA, Culbertson BM (1996). Differential scanning calorimetry (DSC) analyses of superelastic and nonsuperelastic nickel-titanium orthodontic wires. *J. Orthod. Dentofacial Orthop* 190:589-597.
- Jones DA (1992). *Principles and Prevention of Corrosion*, Maxwell Macmillan International Editions 243-291.
- Vrijhoef MMA, Mezger PR, Van der Zel JM, Greener EH (1987). Corrosion of Ferromagnetic Alloys used for Magnetic Retention of Overdentures. *J. Dent. Res* 66:1456-1459.
- ISO 10271, *Dental Metallic Materials: Corrosion test methods*, 2005.